Monte Carlo studies of the band-bending in $GaAs/Al_{0.45}Ga_{0.55}As$ quantum-cascade laser

Jan Konupek,[1] Piotr Borowik,[1] Jean-Luc Thobel[2], and Leszek Adamowicz[*1]

[1]*Faculty of Physics, Warsaw University of Technology, Koszykowa 75, 00-662 Warszawa,*
[2]*Institut d'Électronique, de Microélectronique et de Nanotechnologie, UMR CNRS 8520, Université Lille 1, Avenue Poincaré, BP 69, 59652 Villeneuve d'Ascq Cedex, France*

Received April 09, 2011; accepted April 12, 2011; published June 30, 2011

Abstract—Results of Monte Carlo simulation of mid-infrared QCL structure initially proposed by Page *et al.* [Appl. Phys. Lett. **78**, 3529 (2001)] are presented. The band-bending effect imposed by non-equilibrium electric charge distribution during the laser operation is observed. Perturbations of electric potential, non-equilibrium charge and electron sub-bands populations are demonstrated for a realistic range of electron sheet densities levels.

Electron transport in quantum cascade lasers (QCL) can be successfully described using the Boltzmann Transport Equation (BTE) theory. The transport takes place in the direction perpendicular to the semiconductor hetero-junctions and then can be viewed as a chain of scattering events between discrete sub-bands. In such a picture, the electron states are obtained as solutions of the Schrödinger equation, and then the scattering rates can be obtained using the Born approximation and Fermi Golden Rule. For parallel to hetero-junctions direction, the electron states are modeled as plane waves. Several techniques can be used to calculate the electron sub-band populations and distribution functions. The most popular methods used to solve BTE in QCL structures are: the Monte Carlo (MC) [1-5] and the Rate Equation (RE) [4-8]. Whereas the first one is more general and does not require any additional approximations, the second one assumes that the electron distribution function has the shape of the Fermi-Dirac distribution. In both methods electron interactions with the crystal lattice imperfections as impurities or vibrations – phonons are commonly included.

Also the Coulomb electron interactions play an important role and some research demonstrates that they are needed to obtain population inversion between lasing sub-bands [9]. However, the presence of other electrons in the structure influences the behavior of an electron also in other ways. The first already mentioned is the short-range, the Coulomb type electron-electron interaction [1, 2]. The other type is a more indirect influence of electron gas by screening interactions [2, 10-11], depending on electron density and distribution in the structure. The other one, which we would like to discuss in this paper, is the band-bending effect caused by non-uniform distribution of electrons and ionized impurities along the structure. Such distribution of an electric charge generates additional electrostatic potential which modifies the potential shape determined by the semiconductor material configuration. This leads to position modification of energy sub-bands, corresponding wave-functions and then to modification of electron scattering rates between them. This effect can be included in modeling by solving self-consistently coupled Schrödinger-Poisson equations, where in the Poisson equation the actual electrical charge distribution is used. Our calculations were performed using combined MC and RE algorithm [5] when the RE method is self-consistently coupled to the Schrödinger/ Poisson equation and after reaching the convergence, the MC simulation is executed.

We studied the structure of mid-infrared QCL initially proposed by Page *et al.* [12], and also recently fabricated at ITE, Warsaw [13]. The original device was prepared with an electron sheet density equal to $3.8\times10^{11}cm^{-2}$, but the dependence of the device behavior on the injector doping density was also studied for higher values, as this parameter has a significant influence on understanding the operation and optimization on these devices [14]. Lattice temperature of 150K and electric field conditions of 48kV/cm were assumed for all our studies, as these conditions were reported in [12].

The description of used simulation methods can be found in Ref. [2-5], and the detailed description of the electron microscopic behavior in this structure was presented elsewhere [3].

Although, as will be shown later, the band-bending is also observed for lower densities, in Fig. 1 we present the shape of an electron wave-function in the QCL structures for an electron density of 8×10^{11} cm^{-2} , as obviously for higher densities this effect is clearly visible in the scale of Fig. 1.

* E-mail: adamo@if.pw.edu.pl

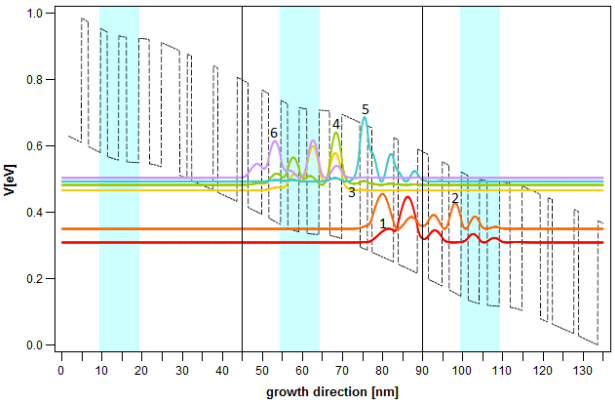

Fig.1. The squares of modules of electron wave-functions and the shape of electric potential shape, calculations for electron sheet density of 8×10^{11} cm^{-2}. Gray areas on the picture indicate positions of doped regions and uniform doping is assumed.

The first observation that we can find when we compare this figure with previously published results [3] is that for higher doping densities the relative position of energy levels changes. In our previous studies, when coupling between the Schrödinger and Poisson equations was neglected, the upper lasing level was the 4th sub-band, and in the presented figure it is the 5th sub-band, when we count the levels from the bottom for only one laser segment. The resonance between these levels can be observed when we change the doping level, and also when we change the applied electric field. However, we do not present or discuss the second effect in this paper. The most visible resonance between these two states is reached for an electron concentration of about $2\cdot10^{11}$cm^{-2}.

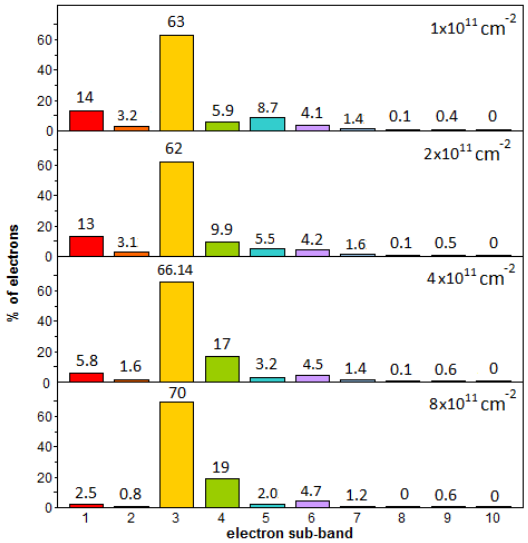

Fig. 2. Sub-band population expressed as % of total number of electrons in the structure. Calculations were performed for 15 sub-bands in the segment, but higher levels were not occupied, so we omit them in this picture.

We can read from Fig.1 that electrons which occupy the 4th level have the wave-functions more overlapping with the doped region than electrons located on the 5th sub-band. This means that lowering the energetic position of the 4th sub-band, in turn, leads to higher population by electrons and finally, to smaller energy of the whole system. The increase of electron population in the 4th level with the increase of electron sheet density can be read from Fig.2.

In the same figure we can also observe that the percentage of electrons on the 1st sub-band decreases with an increase in the electron sheet density. Also, this effect is not surprising when we look at the shapes of its corresponding wave-function. When electrons occupy the first sub-band, it means that their electric charge is located far from the impurities charge. As the doping level increases, the generated internal electric field and potential deformation are stronger. The shape of the potential is bent and the states which do not create such electric charge separation are favored so we can observe proportionally higher electron populations on the 3rd and 4th sub-bands.

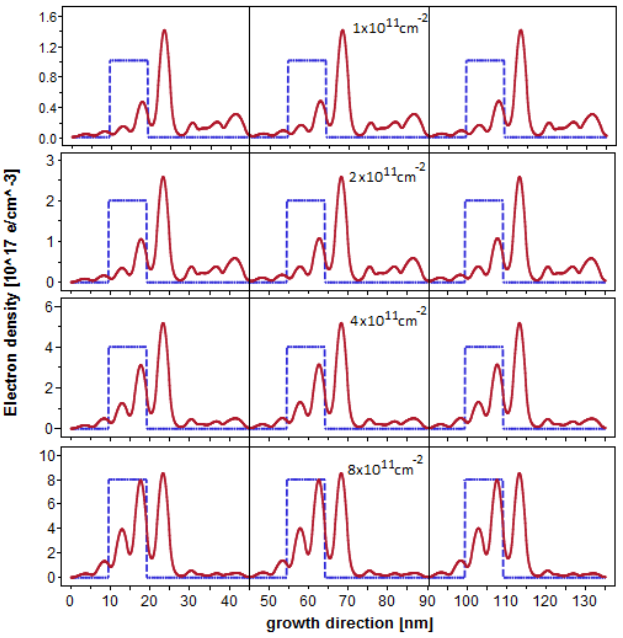

Fig. 3. Shapes of contributions to the electric charge distribution along one segment of the QCL structure. Ionised impurities (dashed line) and electrons (solid line) charge are both plotted as a positive value easier to be compared. The value of a total electric charge is expressed as electrons per cubic cm, which can be easily compared to the doping density. Electrons sheet densities are written in the panels.

The electric charge distribution along the structure is presented in Figs. 3 and 4. As already discussed, with an increase in the doping level, proportionally more electrons are attracted to populate the states which have

their wave-functions more overlapped with the doped region. As a consequence, when we look at individual contributions to the electric charge coming from impurities and electrons part, with electron density increase, the electronic charge tends to be shifted towards the doping region. Also the proportion of the electric charge that is distributed between the doping regions of the neighboring segments is decreased. This may be observed as the flattering of the electrons charge distribution curve in the Fig. 3.

It may be also interesting to look at the overall charge distribution along the structure, which we demonstrate in Fig. 4, together with the electric potential generated by it, and compare the curves for the studied doping levels.

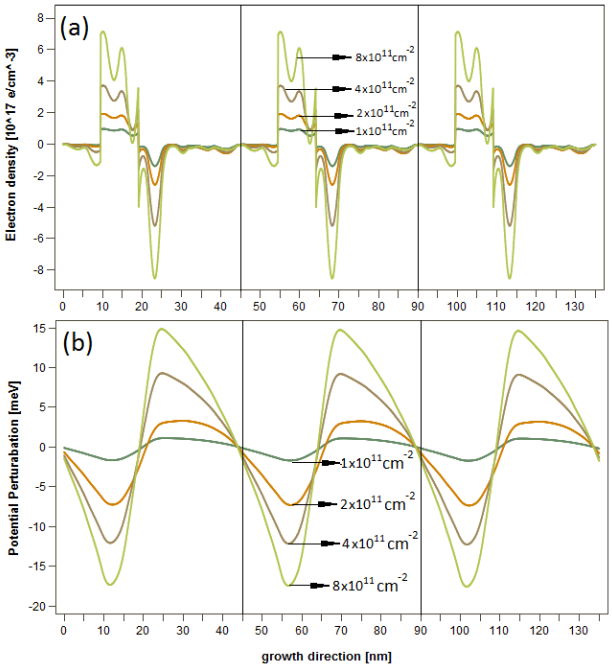

Fig. 4. Overall electric charge distribution along the QCL structure (a), and resulting perturbation of the electrostatic potential (b).

To conclude, the results of the Monte Carlo simulations presented in this paper demonstrate the band-bending effect induced by non-equilibrium charge distribution along the structure of a mid-infrared quantum cascade laser. This effect is visible for realistic doping levels and corresponding electron sheet densities used for the device fabrication. Observed changes of electron states and electron populations can be explained when the shapes of electron wave-functions are examined.

The work was financially supported by grant PBZ-MNiSW-02/I/2007

References

[1] C. Jacoboni and P. Lugli, *The Monte Carlo Method for Semiconductor Device Simulations* (Springer, Wien 1989).
[2] O. Bonno, J.L Thobel, F. Dessenne, J. Appl. Phys. **97**, 043702 (2005).
[3] P. Borowik, J.L. Thobel, L. Adamowicz, J. Appl. Phys. **108**, 073106 (2010).
[4] P. Borowik, J.L. Thobel, L. Adamowicz, Monte Carlo versus Rate Equation studies of population inversion in GaAs/ $Al_{0.45}Ga_{0.55}As$ quantum-cascade laser. (unpublished).
[5] P. Borowik, J.L. Thobel, L. Adamowicz, Combined Rate Equation and Monte Carlo studies of electron populations in quantum-cascade laser. (unpublished).
[6] P. Harrison, Appl. Phys. Lett. **75**, 2800 (1999).
[7] D. Indjin, P. Harrison, R.W. Kelsall, Z. Ikonić, J. Appl. Phys. **91**, 9091 (2002).
[8] K. Donovan, P. Harrison, R.W. Kelsall, J. Appl. Phys. **89**, 3084 (2001).
[9] P. Harrison, R.W. Kelsall, Solid State Electron. **42**, 1449 (1998).
[10] J.T. Lü, J.C. Cao, Appl. Phys. Lett. **89**, 211115 (2006).
[11] R. Nelander, A. Wacker, J. Appl. Phys. **106**, 063115 (2009).
[12] H. Page, C. Becker, A. Robertson, G. Glastre, V. Ortiz, C. Sirtori, Appl. Phys. Lett. **78**, 3529 (2001).
[13] K. Kosiel, M. Bugajski, A. Szerling, J. Kubacka-Traczyk, P. Karbownik, E. Pruszyńska-Karbownik, J. Muszalski, A. Łaszcz, P. Romanowski, M. Wasiak, W. Nakwaski, I. Makarowa, P. Perlin, Phot. Lett. Poland **1**, 16 (2009).
[14] V.D. Jovanović, S. Höfling, D. Indjin, N. Vukmirović, Z. Ikonć, P. Harrison, J.P. Reithmaier, A. Forchel, J. Appl. Phys. **99**, 103106 (2006).

